Human Molecular Genetics, 2012, Vol. 21, No. 2 **300–310**
doi:10.1093/hmg/ddr459
Advance Access published on October 6, 2011

Germline *SDHx* variants modify breast and thyroid cancer risks in Cowden and Cowden-like syndrome via FAD/NAD-dependant destabilization of p53

Ying Ni[1,4], Xin He[1], Jinlian Chen[1], Jessica Moline[1,2], Jessica Mester[1,2], Mohammed S. Orloff[1,2], Matthew D. Ringel[5,6] and Charis Eng[1,2,3,4,7,8,*]

[1]Genomic Medicine Institute, Lerner Research Institute, [2]Taussig Cancer Institute and [3]Stanley Shalom Zielony Nursing Institute, Cleveland Clinic, Cleveland, OH 44195, USA, [4]Howard Hughes Medical Institute Doctoral Program in Molecular Medicine, Department of Molecular Medicine, Cleveland Clinic Lerner College of Medicine of Case Western Reserve University, Cleveland, OH 44106, USA, [5]Division of Endocrinology and Metabolism, Department of Medicine and [6]Comprehensive Cancer Center, Arthur G. James Cancer Hospital and Richard G. Solove Research Institute, The Ohio State University, Columbus, OH 43210, USA, [7]Department of Genetics, Case Western Reserve University School of Medicine, Cleveland, OH 44106, USA and [8]CASE Comprehensive Cancer Center, Case Western Reserve University, Cleveland, OH 44116, USA

Received July 19, 2011; Revised September 19, 2011; Accepted October 3, 2011

Cowden syndrome (CS), a Mendelian autosomal-dominant disorder, predisposes to breast, thyroid and other cancers. Germline mutations in phosphatase and tensin homolog (*PTEN*) have been recently reported in 23% of a large series of classic CS. Here, we validated our small ($n = 10$) pilot study in a large patient series that germline variations in succinate dehydrogenase genes (*SDHx*) occur in 8% (49/608) of *PTEN* mutation-negative CS and CS-like (CSL) individuals (SDH^{var+}). None of these *SDHx* variants was found in 700 population controls ($P < 0.0001$). We then found that *SDHx* variants also occur in 6% (26/444) of *PTEN* mutation-positive ($PTEN^{mut+}$) CS/CSL individuals ($PTEN^{mut+}/SDH^{var+}$). Of 22 $PTEN^{mut+}/SDH^{var+}$ females, 17 had breast cancers compared with 34/105 $PTEN^{mut+}$ ($P < 0.001$) or 27/47 SDH^{var+} patients ($P = 0.06$). Notably, individuals with SDH^{var+} alone had the highest thyroid cancer prevalence (24/47) compared with $PTEN^{mut+}$ patients (27/105, $P = 0.002$) or $PTEN^{mut+}/SDH^{var+}$ carriers (6/22, $P = 0.038$). Patient-derived SDH^{var+} lymphoblastoid cells had elevated cellular reactive oxygen species, highest in $PTEN^{mut+}/SDH^{var+}$ cells, correlating with apoptosis resistance. SDH^{var+} cells showed stabilized and hyperactivated hypoxia inducible factor (HIF)1α signaling. Most interestingly, we also observed the loss of steady-state p53 in the majority of SDH^{var+} cells. This loss of p53 was regulated by MDM2-independent NADH quinone oxidoreductase 1-mediated protein degradation, likely due to the imbalance of flavin adenine dinucleotide/nicotinamide adenine dinucleotide in SDH^{var+} cells. Our data suggest the potential regulation of HIF1α, p53 and PTEN signaling by mitochondrial metabolism in CS/CSL tumorigenesis. Together, our findings suggest the importance of considering *SDHx* as candidate predisposing and modifier genes for CS/CSL-related malignancy risks, and a mechanism which suggests ways of therapeutic reversal or prevention.

INTRODUCTION

Cowden syndrome (CS, [MIM 158350]) is autosomal dominant with lifetime risks of 28% for developing female breast cancer, 10% for epithelial thyroid cancer and unknown but finite risks of developing other cancers (1,2). The syndrome is difficult to recognize because of the protean and variable manifestations of the broad phenotype (2) and remains under-diagnosed. The

*To whom correspondence should be addressed at: Cleveland Clinic Genomic Medicine Institute, 9500 Euclid Avenue, NE-50, Cleveland, OH 44195, USA. Tel: +1 2164443440; Fax: +1 2166360655; Email: engc@ccf.org

incidence of CS was estimated to be 1 in one million (3,4) before gene identification and raised to 1 in 200 000 after (5), which may still be an underestimate. Germline mutations in the phosphatase and tensin homolog deleted on chromosome 10 (*PTEN* [MIM 601728]) tumor suppressor gene were found in up to 85% of CS cases defined by the strict International Cowden Consortium criteria (6), although in a recent series comprising >3000 probands, only 23% of classic CS carry a germline *PTEN* mutation (7). This trend in mutation prevalence with time from initial gene discovery is typical for many heritable syndromes as more probands without family histories and without full phenotype are analyzed, thus making molecular diagnosis difficult and predictive testing challenging, often impossible. When individuals have features of CS but do not meet these criteria, they are referred to as CS-like (CSL) and necessarily represent a heterogeneous series. Only 5% of CSL individuals have germline *PTEN* mutations (8). Thus, illustrative of many cancer syndromes and relevant to clinical practice, other predisposition genes must exist for *PTEN* mutation-negative CS/CSL individuals and families.

Recently, mitochondrial respiratory enzymes have emerged as tumor suppressors, including autosomal genes encoding mitochondrial complex II–succinate dehydrogenase (SDH) (reviewed in 9). Germline homozygous or compound heterozygous mutations in mitochondrial complex genes, including complex II, result in Leigh syndrome, a rare but fatal neurodegenerative disease. Germline heterozygous *SDHB*/*C*/*D* mutations result in hereditary pheochromocytoma–paraganglioma (PCC/PGL) syndrome (10–12). We subsequently noticed a small subset of individuals with germline *SDHB* mutations in our population-based PCC registry also developed early onset renal cell carcinoma (RCC) and papillary thyroid carcinoma, reminiscent of two CS component tumors (12,13). Based on these observations, we carried out a small hypothesis-generating pilot study, which found germline *SDHB* and *SDHD* variants in a subset of CS/CSL individuals without *PTEN* mutations (14). Based on small numbers ($n = 10$), it appeared that germline *SDHx* variant carriers may have elevated frequencies of breast, thyroid and RCC compared with those with germline *PTEN* mutations. It also appeared that the *SDH*-related thyroid cancers were papillary in contrast to *PTEN*-related thyroid cancers whereby follicular histology is over-represented. However, the sample size was small. Functionally, CS/CSL-associated *SDHB* or *SDHD* variants showed similar activation of AKT (protein kinase B) and mitogen-activated protein kinase (MAPK) signaling, which are downstream of the PTEN pathway in a variant-dependent manner, indicating the likely cross-talk between the SDH and PTEN signaling pathways (14).

In the present study, we sought to address our hypotheses that germline *SDHx* variants associate with increased frequencies of component cancers in a large independent series of *PTEN* mutation-negative CS/CSL individuals; and that *SDHx* alleles modify solid tumor risks in individuals with germline *PTEN* mutations. Because the *SDHx* alleles are missense variants, it was important to demonstrate functional relevance. So, we then explored mechanisms whereby *SDHx* variants can lead to tumorigenesis by examining cellular phenotypes such as apoptosis and reactive oxygen species (ROS) status, and candidate dysregulated signaling pathways.

Table 1. List of *SDHx* variants identified in CS/CSL individuals in *PTEN* mutation-negative subset and *PTEN* mutation-positive subset

	Variation	*n*
PTEN mutation-negative subset: (8%, 49/608)		
SDHB ($n = 17$)	c.8C>G, p.Ala3Gly	1
	c.9C>G, p.Arg27Gly	1
	c.170A>G, p.His57Arg	1
	c.359A>G, p.Asn120Ser	1
	c.487T>C, p.Ser163Pro	13
SDHC ($n = 1$)	c.197C>T, p.Ala66Val	1
SDHD ($n = 31$)	c.34G>A, p.Gly12Ser	18
	c.149A>G, p.His50Arg	12
	c.433C>A, p.His145Asn	1
PTEN mutation-positive subset: (6%, 26/444)		
SDHB ($n = 12$)	c.8C>G, p.Ala3Gly	1
	c.158G>A, p.Gly53Glu	1
	c.487T>C, p.Ser163Pro	9
	c.643G>A, p.Ala215Thr	1
SDHD ($N = 14$)	c.34G>A, p.Gly12Ser	3
	c.149A>G, p.His50Arg	11

SDHB RefSeq NM_003000.2.
SDHC RefSeq NM_003001.3.
SDHD RefSeq NM_003002.1.

RESULTS

SDHB/*D* germline variants identified in *PTEN* mutation-negative and *PTEN* mutation-positive CS/CSL patients

Manganese superoxide dismutase (MnSOD) is an indicator of ROS stress and of general mitochondrial dysfunction. Following a similar workflow (Supplementary Material, Fig. S1) as in our pilot paper (14), *PTEN* mutation-negative CS/CSL germline samples with elevated MnSOD levels ($n = 608$, including 10 pediatric patients; Supplementary Material, Table S2) were subjected to *SDHB*/*C*/*D* mutation analysis and their data compared with ancestry-matched controls ($n = 700$). We found 49 of 608 (8%) *PTEN* mutation-negative cases carrying non-synonymous germline *SDHx* mutations/variants (Table 1, upper panel): 17 in *SDHB* [Ala3Gly ($n = 1$), Arg27Gly ($n = 1$), His57Arg ($n = 1$), Asn120Ser ($n = 1$) and Ser163Pro ($n = 13$)], 1 in *SDHC* [Ala66Val] and 31 in *SDHD* [Gly12Ser ($n = 18$), His50Arg ($n = 12$), His145Asn ($n = 1$)]. None of these *SDHx* variants was found in the 700 population controls ($P < 0.0001$).

In order to determine whether *SDHx* variation and *PTEN* mutation are mutually exclusive or can occur together, we examined a nested series of 444 *PTEN* mutation-positive CS/CSL patients (Supplementary Material, Table S2) with germline *PTEN* mutation/variant, including promoter variants and large insertions/deletions, regardless of the MnSOD status. Of the 444, 26 (6%) were also found to carry germline *SDHB*/*D* variants, 12 in *SDHB* [Ala3Gly ($n = 1$), Gly53Glu ($n = 1$), Ser163Pro ($n = 9$), Ala215Thr ($n = 1$)] and 14 in *SDHD* [Gly12Ser ($n = 3$), His50Arg ($n = 11$)] (Table 1, lower panel).

Table 2. Increased cancer frequencies in *SDHx* variant-only carriers and in *PTEN* mutation and *SDHx* variant double-carriers compared with *PTEN* mutation-only carriers

		Breast cancer (/total number)	Thyroid cancer (/total number)	Renal cancer (/total number)
	$PTEN^{mt+}$	34/105 (32.4%)	27/105 (25.7%)	7/105 (6.7%)
	$SDHx^{var+}$	27/47 (57.4%)	24/47 (51.1%)	3/47 (6.4%)
	$PTEN^{mt+}/SDHx^{var+}$	17/22 (77.2%)	6/22 (27.3%)	0
$SDHx^{var+}$ versus $PTEN^{mt+}$	*P*-value	*0.001*	*0.002*	0.28
	OR (95% CI)	2.82 (1.39–5.72)	3.01 (1.47–6.19)	0.95 (0.24–3.87)
$PTEN^{mt+}/SDHx^{var+}$ versus $SDHx^{var+}$	*P*-value	0.06	*0.038*	
	OR (95% CI)	2.52 (0.80–7.98)	0.34 (0.12–1.08)	
$PTEN^{mt+}/SDHx^{var+}$ versus $PTEN^{mt+}$	*P*-value	*<0.001*	0.21	
	OR (95% CI)	7.10 (2.41–20.86)	1.08 (0.39–3.05)	

P-values derived from Fisher's two-tailed exact test. *P*-value <0.05 is considered statistically significant and is in italics. OR, odds ratio; CI, confident interval.

Increased prevalence of breast and thyroid cancers in *SDHx* variant carriers in *PTEN* mutation-negative CS/CSL individuals

The snapshot prevalence of breast, epithelial thyroid and RCC were calculated for the 47 adult individuals carrying *SDHx* variants only (i.e. without *PTEN* mutations). Of the 47 patients with *SDHx* variants, 27 (57.4%) had breast cancer, 24 (51.1%) had epithelial thyroid cancers and 3 (6.4%) RCC (Table 2, upper panel). When compared with patients with only *PTEN* mutations, *SDHx* variant carriers showed odds ratios (OR) of 2.82 (95% CI 1.39–5.72, $P = 0.001$) for breast cancer, and 3.01 (1.47–6.19, $P = 0.002$) for epithelial thyroid carcinoma (Table 2). The prevalence of RCC in *SDHx* variant carriers is similar to *PTEN* mutations carriers. Epithelial thyroid cancers seen in the *SDHx* variant carriers were mostly papillary (22/24, 91%) in histology (majority classic papillary) compared with only one-third among pathogenic *PTEN* mutation carriers ($P < 0.001$).

SDHx alleles associated with modified malignancy risks in *PTEN* mutation carriers

Strikingly, breast cancers developed in 77% (15) of 22 patients carrying both *PTEN* mutations and *SDHx* variants (11 invasive ductal carcinomas and 6 ductal carcinoma *in situ*) when compared with patients with *PTEN* mutations alone (32.4%) [$P < 0.001$; OR = 7.10 (95% CI: 2.41–20.86)], or compared with patients with *SDHx* variants alone (57.4%) [$P = 0.06$, OR = 2.52, (95% CI: 0.80–7.98)]. There were 6 of 22 (27.2%) carriers of both *PTEN* mutation and *SDHx* variant with thyroid cancer compared with 27 of 105 (25.7%) in those with *PTEN* mutations alone [$P = 0.21$, OR = 1.08 (95% CI: 0.39–3.05)] in contrast to 24 of 47 (51.1%) with *SDHx* variants alone [$P = 0.038$, OR = 0.34 (95% CI: 0.12–1.08)]. While the prevalence of thyroid cancer in patients with both *PTEN* mutations and *SDHx* variants is not statistically significantly different from that of *PTEN* mutation-only patients, the histology of these 6 *PTEN*/*SDHx*-related thyroid cancers was exclusively papillary. No RCC were noted in the group with both *PTEN* mutation and *SDHx* variant.

Enhanced apoptosis resistance correlated with elevated ROS in *SDHx* variant carriers

Based on our genotype–phenotype observations above, we hypothesized that the functional consequences of the co-occurrence of *PTEN* and *SDHx* alterations would be more marked, beyond those of *SDHx* alteration alone. To evaluate if *SDHx* variants have any effect in regulating cell death, patient-derived lymphoblastoid cells from controls, *SDHx* variant carriers (SDH^{var+}) and individual samples that have both *SDHx* variant and *PTEN* mutation ($SDH^{var+}/PTEN^{mut+}$) were serum starved overnight and allowed to grow under low serum [0.2% fetal bovine serum (FBS)] conditions for 36 h before measuring the percentage of cells in the sub-G1 cell cycle phase by flow cytometry (Fig. 1A). This revealed a pattern of additive cell death resistance with *SDHx* variants in the presence of *PTEN* mutations. Although some apoptosis resistance was seen in cells with only *SDHx* variants, it was not as pronounced as those with both *PTEN* mutation and *SDHx* variant. ROS marker microscopy revealed significantly increased intracellular ROS levels in representative samples harboring *SDHx* variants compared with normal controls (Fig. 1B), with or without *PTEN* mutation, consistent with our previous finding (14). Quantitative flow cytometry experiments using the same carboxy-H2DCFDA live cell labeling confirmed this observation (Fig. 1C). Interestingly, samples with both *PTEN* mutations and *SDHx* variants showed higher ROS compared with samples with *SDHx* variants alone. Moreover, these observations are inversely correlated with the degree of cell death (Fig. 1A).

Hypoxia inducible factor (HIF)1α stabilized in samples from *SDHx* variant carriers

In SDH-related PCC/PGL syndromes, pseudohypoxia-induced stabilization of hypoxia inducible factor (HIF)1α was hypothesized (16). In order to investigate if the pseudohypoxia hypothesis is also applicable to CS/CSL in the context of PTEN and SDH cross-talk, we analyzed HIF1α protein expression levels in *PTEN* or *SDHx* mutation/variant carriers when compared with normal control samples. *SDHx* variant-positive samples showed increased levels of HIF1α protein compared with controls (Fig. 2A). This result was

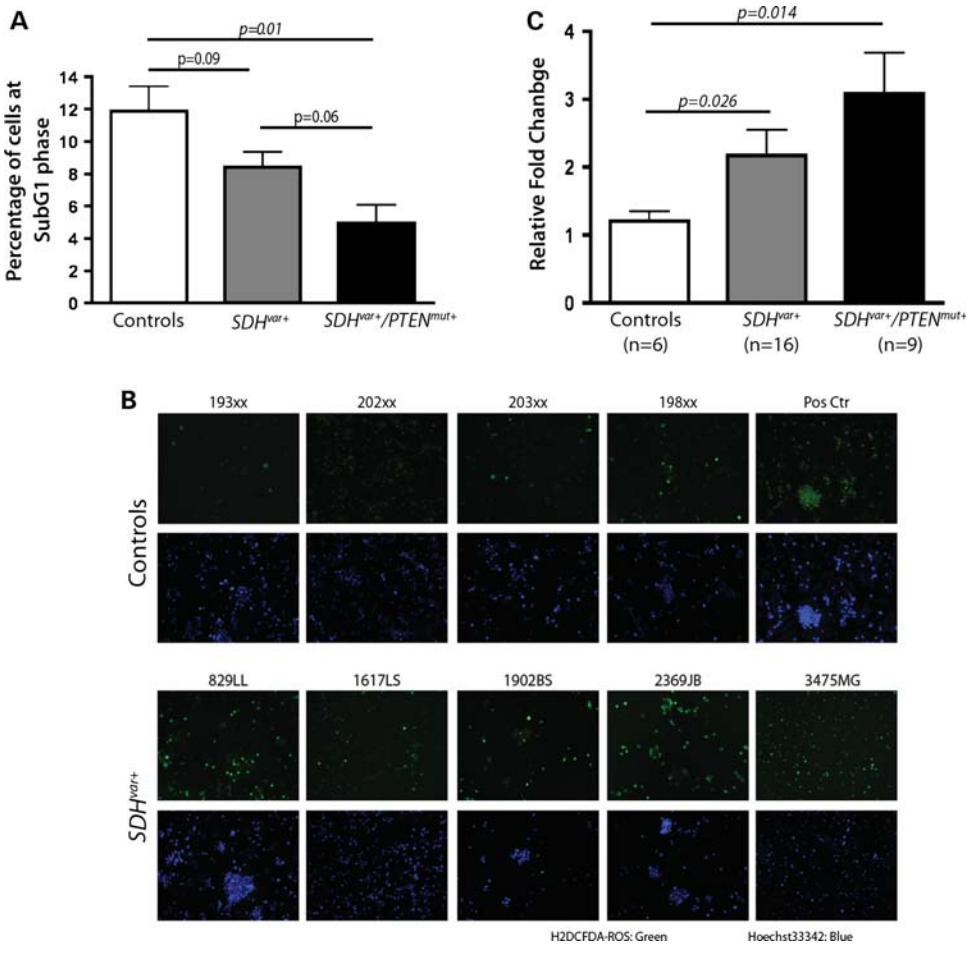

Figure 1. Cellular phenotypes observed in patient cells. (**A**) Cell death is reduced in cells carrying only *SDH* variants (SDH^{var+}) and in samples with both *PTEN* mutation and *SDH* variant ($SDH^{var+}/PTEN^{mut+}$). Note the slight reduction in SDH^{var+} cells in sub-G1 phase compared with control cells and significant reduction in sub-G1 cells from $SDH^{var+}/PTEN^{mut+}$ patients compared with controls (Mean ± SEM). (**B**) Increased intracellular ROS in samples with *SDHx* variants. Representative fluorescent microscopic images with carboxy-H2DCFDA ROS labeling (green) and Hoechst 33342 nuclear labeling (blue). The non-fluorescent 5-(and-6)-carboxy-2′,7′-dichlorodihydrofluorescein diacetate permeates live cells and is deacetylated by non-specific intracellular esterases. In the presence of non-specific ROS, reduced fluorescein compound is oxidized and emits bright green fluorescence. Green dots in figures represent cells with higher cellular ROS. (Upper panel) Four normal control samples (193xx, 202xx, 203xx, 198xx) and one positive control sample treated with ROS inducer *tert*-butyl hydroperoxide (TBHP). (Lower panel) Four CS/CSL patient samples with *SDHx* variants (patient ID—*SDHx* variant: 829LL-S163P, 1902BS-S163P, 1617LS-G12S, 2369JB-S163P) and one PGL patient sample with *SDHB* truncation mutation R46X (3475MG). (**C**) Quantitative ROS measurement by flow cytometry labeling with carboxy-H2DCFDA in normal control, SDH^{var+}, and $SDH^{var+}/PTEN^{mut+}$ groups (mean ± SEM).

confirmed by dot blot analyses (Fig. 2B). *PTEN* nonsense mutation-positive patients showed reduced PTEN protein, while HIF1α protein levels were no different from those of wild-type controls (Fig. 2A). *SDHx* variant-positive samples showed a lower *HIF1A* transcriptional expression relative to samples with *PTEN* mutations (Fig. 2C). In contrast to the protein expression, interestingly, truncating *PTEN* mutations was associated with moderately decreased *HIF1A* transcript and virtually no HIF1α protein. As a confirmation of enhanced HIF1α transactivity due to protein stabilization, one of the well-known HIF1α target genes, vascular endothelial growth factor (VEGF) transcriptional expression was examined using quantitative reverse-transcription polymerase chain reaction (RT–PCR). As shown in Figure 2D, relative *VEGF* mRNA expression was significantly increased in *SDHx* variant carriers compared with normal controls.

Enhanced baseline p53 ubiquitin-independent degradation in *SDHx* variant-positive cells

Exposure of cells to high levels of ROS leads to oxidative stress, and should induce a p53-mediated response including apoptosis, whereas we observed the opposite in our cases. Therefore, we decided to investigate if p53 is somehow modified in our patient samples in order to escape the expected apoptotic regulation. Western blots showed reduced p53 protein expression in the majority of samples harboring *SDHx* variants compared with normal controls (Fig. 3A and B, upper panels). In contrast to p53 protein levels, *TP53* mRNA expression was not changed in *SDHx* variant-positive samples compared with controls (Fig. 3C), suggesting that the loss of p53 protein was not from down-regulated *TP53* transcript. Cells treated with proteasome inhibitor MG132

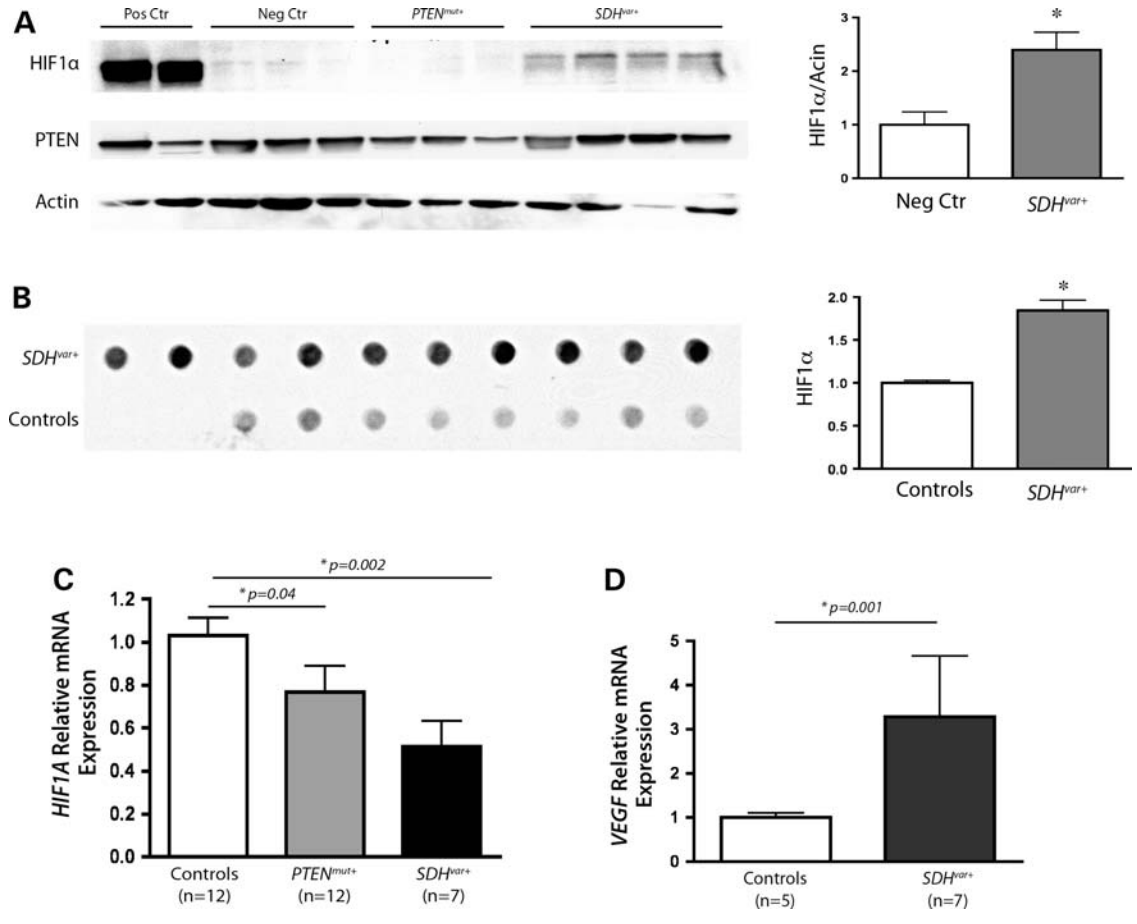

Figure 2. HIF1α protein stabilized with accumulation in *SDHx* variant-positive samples. (**A**) Western blot analysis of HIF1α, PTEN and β-actin protein expression in *PTEN* mutation-positive, *SDHx* variant-positive patients including (patient ID—*SDHx* variant): 826GV-H50R, 1617LS-G12S, 1902BS-S163P, 2369JB-S163P, positive controls (Pos Ctr, samples stimulated with $CoCl_2$ to mimic hypoxia condition) and normal (Neg Ctr) controls. Relative levels of HIF1α protein were quantitated by densitometry and normalized to β-actin in right panel. Results are fold change in SDH^{var+} carriers compared with normal control cells. (**B**) A dot blot analysis of HIF1α protein expression in SDH^{var+} samples and controls. Relative levels of HIF1α protein were quantitated by densitometry in right panel. Results are fold change in SDH^{var+} carriers compared with normal control cells. (**C**) Relative HIF1α mRNA expressions in *PTEN* mutation-positive and *SDHx* variant-positive patients compared with normal controls. (**D**) Relative VEGF mRNA expression is upregulated in *SDHx* variant-positive samples. Data were presented as (Mean ± SEM). $^*P < 0.05$.

abolished the loss of the p53 protein phenomenon in *SDHx* variant-positive cells (Fig. 3A and B, lower panels), indicating that the loss of p53 protein is most likely due to enhanced protein degradation. The multiple bands >53 kDa are likely ubiquitinated p53 resulting from proteasomal inhibition.

To further explore the regulation of p53 degradation, we then investigated the main MDM2-related proteasomal degradation pathway (15,17). No corresponding increase in MDM2 or p-MDM2 was observed (Supplementary Material, Fig. S2A). Because NADH quinone oxidoreductase 1 (NQO1) has been shown to bind and stabilize p53 through MDM-independent pathways (18–20), we next checked the NQO1 status in our control and patient cell lines with the hypothesis that either absolute levels of NQO1 could be reduced or the interaction between NQO1 and p53 could be disrupted in the presence of *SDHx* variation. First, we did not observe obvious decreases of NQO1 expression (Supplementary Material, Fig. S2B) in *SDHx* variant-positive cells, indicating that decreased p53 protein was not a consequence of decreased NQO1 expression. Secondly, dose-dependent induction of NQO1 by NQO1 inducer dimethyl fumarate (DMF) treatment had no significant impact on either p53 protein expression or cell apoptosis in *SDHx* variant-positive cells either (Supplementary Material, Figs S2C and S2D), indicating that NQO1 induction cannot rescue the *SDHx* variant-associated loss of p53. Finally and importantly, co-immunoprecipitation experiments showed decreased binding between NQO1 and p53 in *SDHx* variant-positive patient cells compared with controls (Fig. 3D), suggesting that the loss of p53 is indeed caused by defective interactions between NQO1 and p53.

Altered flavin adenine dinucleotide (FAD) and nicotinamide adenine dinucleotide (NAD) concentrations in *SDHx* variant carrier samples

We then hypothesized that the impaired binding between NQO1 and p53 may be caused by accumulated flavin adenine dinucleotide (FAD), which is a cofactor for both NQO1 and SDH enzymatic activity. To test this hypothesis, FAD and nicotinamide adenine dinucleotide (NAD)+/

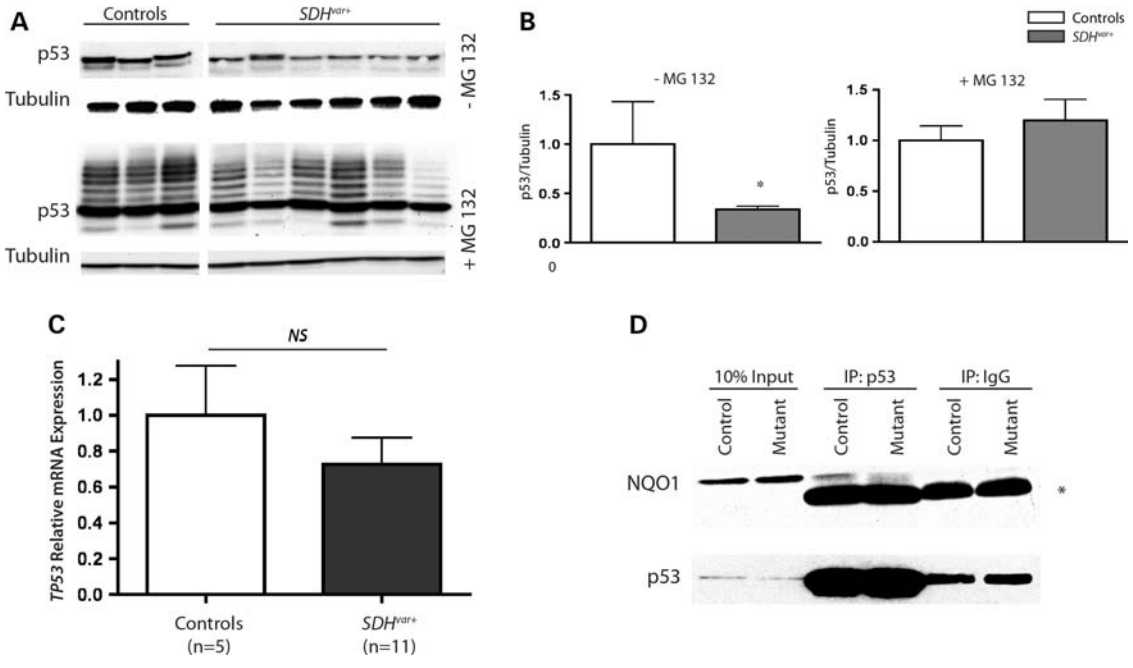

Figure 3. p53 expression at both the protein and mRNA level. (**A**) Western blot of p53 protein in *SDHx* variant-positive CS/CSL (patient ID—*SDHx* variant: 829LL-S163P, 1965ML-S163P, 2094GR-H50R, 2549MP-G12S, 2854PS-S163P, 2894KP-H50R) and normal control groups. Upper panel shows the protein profile under normal culture condition, and lower panel after cells treated with 4 μM proteasomal inhibitor MG132 for 4 h. Tubulin served as a loading control in both conditions. (**B**) Relative levels of p53 were quantitated by densitometry and normalized to tubulin. Results are fold change compared with normal control cells, with (upper panel) or without MG132 treatment (lower panel). Data were presented as (mean ± SEM). $^*P < 0.05$. (**C**) Relative TP53 mRNA expression by quantitative RT–PCR in *SDHx* variant-positive samples compared with normal controls, with glyceraldehyde 3-phosphate dehydrogenase (GAPDH) as internal control. (**D**) Immunoprecipitation of p53 from control and SDH^{var+} LCL whole-cell lysate blotting for NQO1 and p53, *indicates the light chain band of IgG.

NADH (as product/substrate of NQO1) concentrations were measured directly in control and *SDHx* variant carrier lymphoblastoid cells. Indeed, we observed elevated FAD level in *SDHx* variant-positive cells compared with controls (Fig. 4A, left panel). In contrast to higher FAD levels, NAD+ was lower in *SDHx* variant-positive cells with no change in NADH (Fig. 4A, middle and right panels). When we supplemented normal control cells with an excess (250 μM) of riboflavin (FAD precursor) for 48 h, significant reductions in NAD+ levels (Fig. 4B) were also detected, but not NADH, and were accompanied by increased cellular FAD. This is consistent with our observations in *SDHx* variant-positive patient cells. More interestingly, FAD-treated control cells showed similar reductions in p53 expression (Fig. 4C), mirroring our observations in non-FAD-treated patients cells carrying *SDHx* variants (above). FAD treatment of control cells resulted in increased p-AKT and p-MAPK activation, mimicking the inactivation of the PTEN pathway, without changing PTEN protein expression.

DISCUSSION

Individuals with heritable cancer syndromes, such as CS/CSL, who do not carry mutations in the known predisposition genes, bring challenges to molecular diagnosis, predictive testing of family members, genetic counseling and preventive medical management. Identifying additional cancer susceptibility genes for CS/CSL would improve and facilitate the gene-specific personalized medical care. We have recently uncovered an alternative mechanism, germline hypermethylation of the tumor suppressor gene *KLLN* (encoding KILLIN), accounting for one-third of *PTEN* mutation-negative CS/CSL (21). Germline *KLLN* hypermethylation is associated with increased risks of breast and renal cancers over those with *PTEN* mutations. Our current study not only validates the previous pilot observations that *SDHx* variants occur in ~8% of *PTEN* mutation-negative CS/CSL patients, but also validates the elevated breast and thyroid cancer frequencies over those with *PTEN* mutations. *SDHx*, together with *PTEN* and *KLLN*, may form a panel of predisposition genes considered for genetic testing for CS/CSL, perhaps prioritized based on the individual patient's clinical phenotype at presentation and their family history. For example, if a CS/CSL individual has papillary thyroid carcinoma, then *SDHx* testing should be considered first.

As with all inherited cancer syndromes to date, while we can counsel increased prevalence of specific cancers, we cannot predict which subset of those with *PTEN* mutations will develop each component cancer. Here we have found that 6% of *PTEN* mutation/variant-positive CS/CSL patients were also found to have germline *SDHx* variants, and the presence of *SDHx* variants appear to further modify *PTEN* mutation cancer risks over those of *PTEN* mutation in isolation. Because this is the first observation of *SDHx* variation modifying *PTEN*-related breast cancer risk, this will need to be independently validated before translation into the routine clinical armamentarium.

Among all 11 different *SDHx* variants we detected, there are 4 novel variants not previously reported in either NCBI SNP

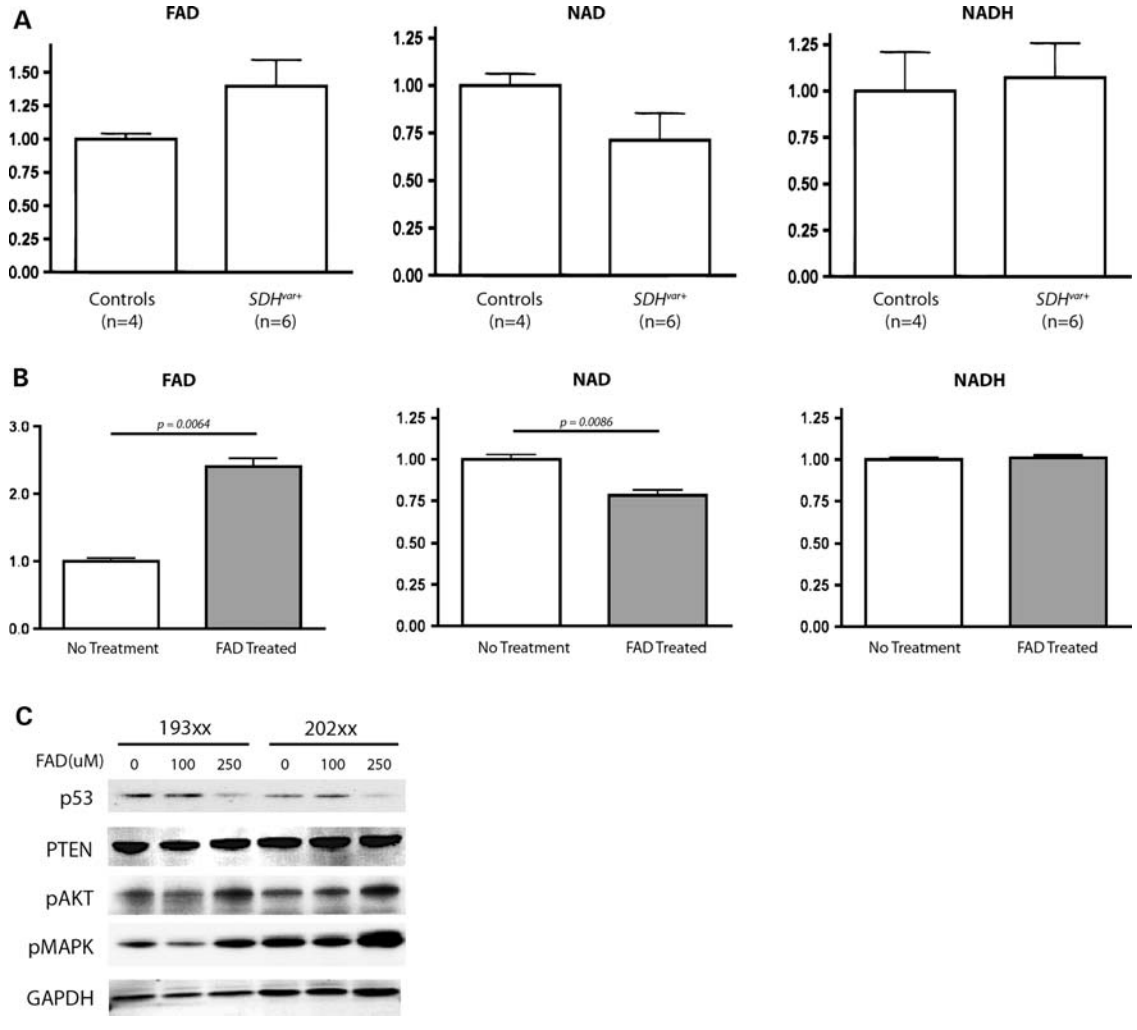

Figure 4. Altered FAD/NAD levels in cells linked to p53 downregulation. (**A**) Nomalized FAD, NAD, NADH measurements in control and SDH^{var+} cells. (**B**) Normalized FAD, NAD, NADH measurements in four control cell lines with or without 250 μM FAD treatment for 48 h. (**C**) Two control cell lines were treated with either 100 or 250 μM FAD for 48 h. Whole-cell lysate then was blotted for p53, PTEN, p-AKT, p-MAPK and GAPDH as loading control.

database (http://www.ncbi.nlm.nih.gov/snp/) or *SDHx* mutation database (http://chromium.liacs.nl/lovd_sdh), *SDHB* Arg27Gly, Asn120Ser, Ala215Thr and *SDHC* Ala66Val. *SDHC* Ala66Val detected represents the first *SDHC* variant in a CSL patient, a 54-year-old patient with invasive breast cancer, follicular thyroid cancer, uterine fibroids and skin hemangioma. Patients with *SDHB* Arg27Gly, Asn120Ser or Ala215Thr variants all presented with invasive breast carcinoma and either malignant (papillary thyroid cancer) or benign thyroid lesions. The other patient with *SDHD* His145Asn (rs121908984) variant first reported in our previous pilot study presented with both breast carcinoma and RCC. The fact that carriers of these variants all presented with malignant breast carcinoma suggest physiologic relevance. *SDHB* Ala3Gly (rs11203289) and His57Arg (rs35962811) were reported in dbSNP but only in African American population, while our samples are derived from white individuals of European ancestry. The most frequent variants *SDHB* Ser163Pro (rs33927012), *SDHD* Gly12Ser (rs34677591) and *SDHD* His50Arg (rs11214077) we seen in our CS/CSL individuals have also been reported in the database. Although these relatively common (1–5% frequency) variants were computationally predicted to be functionally benign (22), our experimental data provide molecular evidence that they could have functional impact in cellular signaling regulation as well. The reason why bioinformatic analysis of prediction fails in *SDHx* genes is because they are extremely well conserved throughout species (23). With enormous numbers of variations uncovered by whole genome sequencing, it is essential to realize that functional analysis and clinical correlations must be performed to define the true pathogenic effect of DNA variations (24), as we have done in the current study.

Changes in the mitochondrial metabolism have long been linked to cancer, known as the Warburg effect (25). The mechanism(s) of disruption of mitochondrial function leading to neoplasia remain unclear. Succinate, the substrate of SDH, may function as a second messenger between the mitochondria (energy production body) and cytosol. Accumulation of succinate due to *SDHx* mutations inhibit

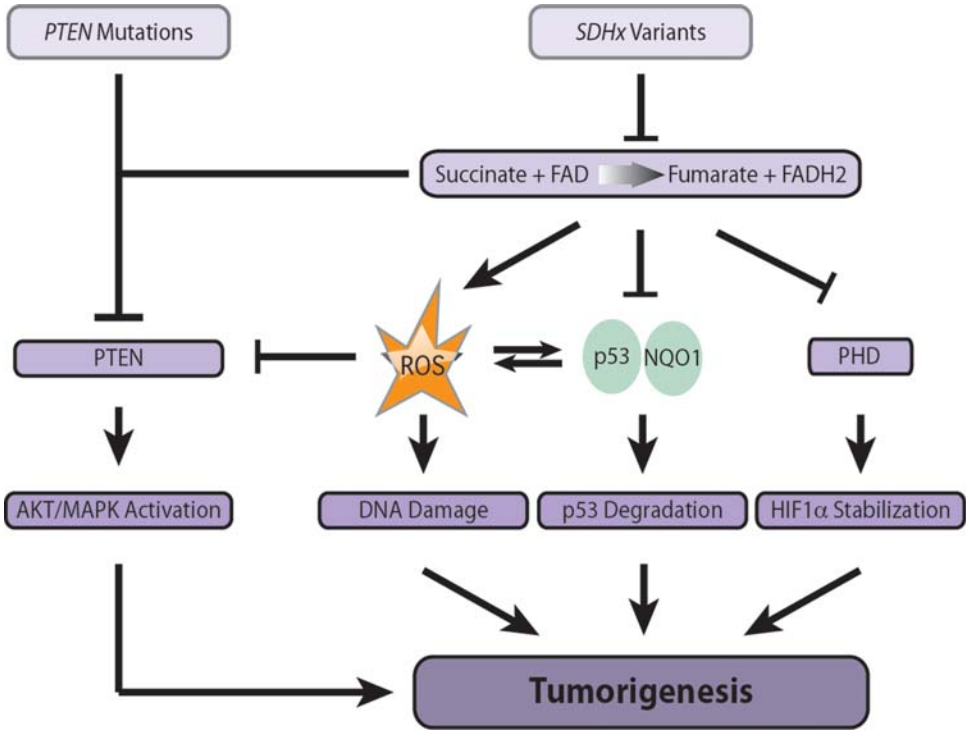

Figure 5. Proposed signaling model of CS/CSL tumorigenesis caused by *SDHx* variants.

the prolyl-hydroxylase enzyme and contributes to stabilization of HIF1α in turn promoting transcription of genes containing hypoxic response elements believed to promote cancer (16). Our data suggest that the hyperactivation of the HIF pathway is indeed involved in our CS/CSL development. It has been reported that the HIF signaling pathway can also be regulated by AKT and mTOR signaling downstream of PTEN (26). It is notable that HIF1α expression in *PTEN* mutation-positive samples versus *SDHx* variant-only samples are different. We observed no obvious accumulation of HIF1α protein with *PTEN* mutation, consistent with other reports that loss of function of PTEN most likely increases the HIF1α transactivation function by preventing HIF1α binding to HIF inhibitory factor (FIH), instead of stabilizing HIF1α protein expression (27). This contrasts with our observation of *SDHx*-related hyperactivation of HIF1α. This differential involvement of HIF signaling may partially explain the different levels of predisposition to breast, thyroid and/or renal carcinomas in *PTEN* mutation positive or *SDHx* variant positive, versus both.

As 'energy factories' through oxidative phosphorylation, mitochondria make endogenous ROS as byproducts of normal respiration. Under normal physiological conditions, complex II is not considered to be a site for ROS generation. However, the structure–function studies of bacterial Sdh and fumarate dehydrogenase indicated ROS production mainly resides at the FAD site of these enzymes (28). The succinate-driven reverse-electron transfer through complex I was shown as another mechanism to yield the highest rates of H_2O_2 in isolated mitochondria (29). Therefore, accumulated succinate from dysfunctional SDH complex not only could serve as a second messenger activating HIF signaling (as discussed above), but also could drive the intracellular ROS generation. The extra ROS stress has been reported with *SDHx* mutations (30), and also observed in our *SDHx* variant carrier cells in general. Certain *PTEN* mutation-positive cells do show elevated ROS (31), which accounts for the additive increased ROS in samples with both *PTEN* mutation and *SDHx* variant. Excessive oxidation of DNA by ROS could be a major cause of DNA damage and genetic instability (32,33), which leads to accumulation of mutations and deletions that eventually contribute to carcinogenesis.

TP53, as a stress-induced tumor suppressor gene, plays important roles in programmed cell death (34). The reduction in basal p53 levels in *SDHx* variant carriers likely explains the corresponding escape of cell death, which otherwise should be regulated by the p53 pathway under normal cellular responses. A recent study also suggested that mitochondrial respiration deficiency may impair p53 expression and function (35), which is consistent with our observation. We further investigated the underlying mechanism of this p53 impairment caused by *SDHx* variation. The tightly regulated p53 protein levels are achieved via both ubiquitin-mediated degradation in 26S proteasomes based on interactions between p53 and Mdm2 (36), and an ubiquitin-independent degradation in 20S proteasomes (18–20,37). In the latter, p53 is degraded by 20S proteasomes through direct binding to NQO1. What is intriguing to us is that the function of NQO1 is tightly regulated by mitochondrial redox metabolites. As a key player here, NQO1 is a FAD-containing protein and its activity is highly dependent on intracellular NAD^+/NADH, also the product and substrate, respectively, of mitochondrial complex I (38). Our data suggest that in our *SDHx* variant cells, it is not the loss of absolute NQO1 expression but

more specifically the loss of functional NQO1 binding to p53 that results in the reduction in p53 protein. The observation that increased FAD and lowered NAD+ concentrations in *SDHx* variant cells validates the observation of inhibited NQO1 function. Presence of excessive FAD results in activated signaling down the AKT and MAPK pathways, mimicking PTEN dysfunction. Therefore, our findings reveal a novel mechanism that mitochondrial metabolites regulate cellular signaling, hence mechanistically linking mitochondrial dysfunction to tumorigenesis.

In conclusion, our genetic analyses revealed that germline *SDHx* variants are associated with elevated cancer risks in CS/CSL individuals, both alone and synergistically with germline *PTEN* mutations. Our functional data suggest that disruption of complex II could lead to mitochondrial metabolite imbalance, and in turn cause the stabilization of HIF1α, loss of baseline p53 levels and is at least partially responsible for ROS generation. The cross-talk between SDH and PTEN results in a multi-signaling cascade that contributes to tumorigenesis (Fig. 5). As we are learning more about the heterogeneity of tumor formation, it is not surprising to observe multiple pathways crosstalk, contribute alone or simultaneously to the final outcome of differential organ-specific carcinogenesis. Together, our findings suggest the importance of considering *SDHx* as candidate predisposing genes and as candidate modifier genes for CS/CSL-related malignancy risks, and may also guide future tailored preventative or therapeutic approaches.

MATERIALS AND METHODS

Subjects and germline DNA extraction

CS or CSL patients were prospectively enrolled in accordance with our research protocol IRB8458-PTEN, which was approved by the Cleveland Clinic and respective Institutional Review Boards for Human Subjects Protection. All research participants provided written informed consent. To be enrolled in the IRB8458-PTEN, individuals are eligible if he/she meets the full CS diagnostic criteria established by the International Cowden Consortium (Supplementary Material, Table S1) or the relaxed criteria (criteria minus one) according to version 2006 NCCN Guidelines (39). Patients meeting the relaxed criteria are referred to as individuals with CSL phenotypes or CSL. In other words, CSL was diagnosed when an individual did not fully meet the strict diagnostic criteria but had features with one or two criteria short of the operational diagnostic criteria. Matching the subjects, normal (population) controls are from northern and western European origin and were anonymized prior to storage and analysis.

Germline DNA was extracted from peripheral blood samples from patients and healthy controls by the Genomic Medicine Biorepository (GMB), Genomic Medicine Institute, Cleveland Clinic (protocols are available at GMB website, http://www.lerner.ccf.org/gmi/gmb/methods.php).

Lightscanner and sequencing for mutation scanning

Genomic DNA was first analyzed using high-resolution melting LightScanner technology (Idaho Technology Inc., Salt Lake City, UT, USA), which detects nucleic acid sequence variations, by changes in the melting curve. Primers to amplify a total of 20 amplicons spanning the exons, exon–intron junctions and flanking intronic regions as well as promoters of *SDHB*/*C*/*D* were designed using LightScanner Primer Design software (all primers are listed in Supplementary Material, Table S3) and optimized according to the manufacturer's instructions. Germline genomic DNA samples were amplified with LCGreen® Plus (Idaho Technology) in a final reaction volume of 10 μl with 20 μl oil overlay. The temperature cycling protocol consisted of an initial denaturation step at 95°C for 2 min, followed by 37 cycles of denaturation at 94°C for 30 s, optimal annealing temperature for each amplicon for 30 s and heteroduplex formation step at 95°C for 30 s and final hold at 25°C. Melting curve analysis was performed on LightScanner with LightScanner software employing three steps, namely, normalization, temperature shift and generating difference plot to cluster samples. Samples with melting curves that clustered differently from reference samples were directly sequenced for *SDHB*, *SDHC* or *SDHD*, as previously reported by our laboratory (40,41).

Cell lines and cell cultures

Human immortalized lyphoblastoid cell lines (LCLs) derived from patients and controls were generated by Genomic Medicine Biorepository, Genomic Medicine Institute, Cleveland Clinic (protocols are available at GMB website, http://www.lerner.ccf.org/gmi/gmb/methods.php). LCLs were cultured in RPMI 1640 supplemented with 20% FBS and 100 units/ml each of penicillin and streptomycin. All cell lines were cultured at 37°C with 5% CO_2. NQO1 inducer DMF (Sigma-Aldrich Co., St Louis, MO, USA) was added into cell culture at different doses as described in figure legend.

RNA extraction and quantitative reverse-transcription–PCR

Total RNA was extracted from LCLs from controls and patients using RNeasy® Mini Kit (QIAGEN, Inc., Valencia, CA, USA) according to the manufacturer's protocol, and subsequently treated with DNase I (Invitrogen, Carlsbad, CA, USA). DNase-treated total RNA from each LCL was reverse-transcribed into cDNA using random primers and SuperTranscript™ III Reverse Transcriptase (Invitrogen), as specified by the manufacturer. PCR was performed using SYBR Green PCR Master Mix and run on 7500 Real Time PCR machine (Applied Biosystem, Carlsbad, CA, USA) using the following intron-spanning primers: 5′-GAAAAAGATAAGTTCTGAACGTCGAA-3′ and 5′-CCTTATCAAGATGCGAACTCACA-3′ for HIF1A; 5′-CTACCTCCACCATGCCAAGTG-3′ and 5′-TGATTCTG CCCTCCTCCTTCT-3′ for VEGF; 5′-CTGTCCCTTCCCAG AAAACCT-3′ and 5′-GGGAGTACGTGCAAGTCACAGA-3′ for P53; 5′-GGGCTGCTTTTAACTCTGGTAA-3′ and 5′-A TGGGTGGAATCATATTGGAAC-3′ for GAPDH.

Protein analysis

Whole-cell lysates were prepared as described before (42) with M-PER Mammalian Protein Extraction Reagent (ThermoFisher Scientific, Waltham, MA, USA) supplemented

with protease inhibitor cocktail and phosphatase inhibitor cocktail (Sigma-Aldrich). Lysates were either separated by sodium dodecyl sulfate polyacrylamide gel electrophoresis and transferred to nitrocellulose or applied to nitrocellulose with a dot blot apparatus (BioRad, Hercules, CA, USA). The resulting blots were subjected to western blot analysis for PTEN (6H2.1, Cascade Bioscience, Portland, OR, USA), MnSOD (Upstate Biotechnology, Waltham, MA, USA), HIF1α (BD Biosciences, San Jose, CA, USA), p53, Actin (Santa Cruz Biotechnology, Santa Cruz, CA, USA) and α-tubulin (Sigma-Aldrich) protein levels.

ROS measurement

The measurement of ROS was performed using carboxy-dichlorodihydrofluorescein diacetate (Carboxy-H2DCFDA), a reliable fluorogenic marker for ROS in live cells (Molecular Probes, Invitrogen). The cells were washed with HBSS/Ca/Mg buffer, centrifuged, resuspended in HBSS/Ca/Mg and incubated with 25 μM carboxy-H2DCFDA for 30 min at 37°C. Hoechst 33342 was added at a final concentration of 1 μM to the carboxy-H2DCFDA staining solution during the last 5 min of the incubation. Fluorescence imaging was taken immediately after washing and mounting the samples. For flow cytometry measurement, cells were washed and resuspended in HBSS/Ca/Mg buffer after incubation and count with FACScans (Becton-Dickinson) immediately.

Cell cycle analysis by FACS flow cytometry

LCLs were serum starved overnight and allowed to grow under 0.2% FBS condition for 36 h before 70% ethanol fixation for cell cycle analysis using FACScan flow cytometer (Becton-Dickinson).

FAD, NAD+/NADH quantification

FAD concentration was measured using FAD assay kit #357-100 (BioVision, Mountain View, CA, USA) following product protocol. In brief, cells were homogenized and deproteinized. Samples and FAD standard were incubated with FAD enzyme mix, OxiRed Probe and assay buffer for 15–60 min in duplicates before measured by the colorimetric method ($\lambda = 570$ nm).

NAD and NADH concentrations were measured using NAD+/NADH quantification kit #337-100 (BioVision) following product protocol. In brief, cells were extracted by freeze/thaw two cycles (20 min on dry ice, then 10 min at room temperature). Extracted samples were filtered through 10 kDa molecular weight cut off filters (BioVison #1997-25) to remove enzymes consuming NADH before performing the assay. To detect total NADt (NADH and NAD), the samples and NADH standard were incubated directly with NAD cycling mix (cycling buffer and enzyme mix). To detect NADH, samples were heated to 60°C for 30 min to decompose NAD before incubating with NAD cycling mix. Duplicated samples were then mixed with NADH developer and incubated at room temperature for 1–4 h before colorimetric reading at OD 450 nm. The amount of NAD in samples was calculated by subtracting NADH from NADt.

Statistical analysis

The frequency of each of the carcinomas in *SDHx* variant-positive individuals were compared with that in a cohort of 105 *PTEN* mutation-positive individuals with the CS/CSL phenotype. Fisher's two-tailed exact test was applied with the significance at $P < 0.05$.

SUPPLEMENTARY MATERIAL

Supplementary Material is available at *HMG* online.

Conflict of Interest statement. None declared.

FUNDING

This work was funded, in part, by the National Cancer Institute (P01CA124570 to C.E. and M.D.R.), the Breast Cancer Research Foundation (to C.E.) and the William Randolf Hearst Foundations (to C.E.). Y.N. is a recipient of the USARMC Department of Defense Breast Cancer Research Program Predoctoral Fellowship (W81XWH-10-1-0088). C.E. is the Sondra J. and Stephen R. Hardis Chair of Cancer Genomic Medicine at the Cleveland Clinic, and is an American Cancer Society Clinical Research Professor, generously funded, in part, by the F.M. Kirby Foundation. Funding to pay the Open Access publication charges for this article was provided by the Cleveland Clinic.

REFERENCES

1. Eng, C. (2003) PTEN: one gene, many syndromes. *Hum. Mutat.*, **22**, 183–198.
2. Zbuk, K.M. and Eng, C. (2007) Cancer phenomics: RET and PTEN as illustrative models. *Nat. Rev. Cancer*, **7**, 35–45.
3. Nelen, M.R., Padberg, G.W., Peeters, E.A., Lin, A.Y., van den Helm, B., Frants, R.R., Coulon, V., Goldstein, A.M., van Reen, M.M., Easton, D.F. *et al.* (1996) Localization of the gene for Cowden disease to chromosome 10q22-23. *Nat. Genet.*, **13**, 114–116.
4. Starink, T.M., van der Veen, J.P., Arwert, F., de Waal, L.P., de Lange, G.G., Gille, J.J. and Eriksson, A.W. (1986) The Cowden syndrome: a clinical and genetic study in 21 patients. *Clin. Genet.*, **29**, 222–233.
5. Nelen, M.R., Kremer, H., Konings, I.B., Schoute, F., van Essen, A.J., Koch, R., Woods, C.G., Fryns, J.P., Hamel, B., Hoefsloot, L.H. *et al.* (1999) Novel PTEN mutations in patients with Cowden disease: absence of clear genotype-phenotype correlations. *Eur. J. Hum. Genet.*, **7**, 267–273.
6. Marsh, D.J., Coulon, V., Lunetta, K.L., Rocca-Serra, P., Dahia, P.L., Zheng, Z., Liaw, D., Caron, S., Duboue, B., Lin, A.Y. *et al.* (1998) Mutation spectrum and genotype-phenotype analyses in Cowden disease and Bannayan-Zonana syndrome, two hamartoma syndromes with germline PTEN mutation. *Hum. Mol. Genet.*, **7**, 507–515.
7. Tan, M.H., Mester, J., Peterson, C., Yang, Y., Chen, J.L., Rybicki, L.A., Milas, K., Pederson, H., Remzi, B., Orloff, M.S. *et al.* (2011) A clinical scoring system for selection of patients for PTEN mutation testing is proposed on the basis of a prospective study of 3042 probands. *Am. J. Hum. Genet.*, **88**, 42–56.
8. Marsh, D.J., Dahia, P.L., Caron, S., Kum, J.B., Frayling, I.M., Tomlinson, I.P., Hughes, K.S., Eeles, R.A., Hodgson, S.V., Murday, V.A. *et al.* (1998) Germline PTEN mutations in Cowden syndrome-like families. *J. Med. Genet.*, **35**, 881–885.
9. Eng, C., Kiuru, M., Fernandez, M.J. and Aaltonen, L.A. (2003) A role for mitochondrial enzymes in inherited neoplasia and beyond. *Nat. Rev. Cancer*, **3**, 193–202.
10. Baysal, B.E., Ferrell, R.E., Willett-Brozick, J.E., Lawrence, E.C., Myssiorek, D., Bosch, A., van der Mey, A., Taschner, P.E., Rubinstein,

W.S., Myers, E.N. *et al.* (2000) Mutations in SDHD, a mitochondrial complex II gene, in hereditary paraganglioma. *Science*, **287**, 848–851.
11. Neumann, H.P., Bausch, B., McWhinney, S.R., Bender, B.U., Gimm, O., Franke, G., Schipper, J., Klisch, J., Altehoefer, C., Zerres, K. *et al.* (2002) Germ-line mutations in nonsyndromic pheochromocytoma. *N. Engl. J. Med.*, **346**, 1459–1466.
12. Neumann, H.P., Pawlu, C., Peczkowska, M., Bausch, B., McWhinney, S.R., Muresan, M., Buchta, M., Franke, G., Klisch, J., Bley, T.A. *et al.* (2004) Distinct clinical features of paraganglioma syndromes associated with SDHB and SDHD gene mutations. *JAMA*, **292**, 943–951.
13. Vanharanta, S., Buchta, M., McWhinney, S.R., Virta, S.K., Peczkowska, M., Morrison, C.D., Lehtonen, R., Januszewicz, A., Jarvinen, H., Juhola, M. *et al.* (2004) Early-onset renal cell carcinoma as a novel extraparaganglial component of SDHB-associated heritable paraganglioma. *Am. J. Hum. Genet.*, **74**, 153–159.
14. Ni, Y., Zbuk, K.M., Sadler, T., Patocs, A., Lobo, G., Edelman, E., Platzer, P., Orloff, M.S., Waite, K.A. and Eng, C. (2008) Germline mutations and variants in the succinate dehydrogenase genes in Cowden and Cowden-like syndromes. *Am. J. Hum. Genet.*, **83**, 261–268.
15. Kubbutat, M.H., Jones, S.N. and Vousden, K.H. (1997) Regulation of p53 stability by Mdm2. *Nature*, **387**, 299–303.
16. Selak, M.A., Armour, S.M., MacKenzie, E.D., Boulahbel, H., Watson, D.G., Mansfield, K.D., Pan, Y., Simon, M.C., Thompson, C.B. and Gottlieb, E. (2005) Succinate links TCA cycle dysfunction to oncogenesis by inhibiting HIF-alpha prolyl hydroxylase. *Cancer Cell*, **7**, 77–85.
17. Haupt, Y., Maya, R., Kazaz, A. and Oren, M. (1997) Mdm2 promotes the rapid degradation of p53. *Nature*, **387**, 296–299.
18. Asher, G., Lotem, J., Cohen, B., Sachs, L. and Shaul, Y. (2001) Regulation of p53 stability and p53-dependent apoptosis by NADH quinone oxidoreductase 1. *Proc. Natl Acad. Sci. USA*, **98**, 1188–1193.
19. Asher, G., Lotem, J., Kama, R., Sachs, L. and Shaul, Y. (2002) NQO1 stabilizes p53 through a distinct pathway. *Proc. Natl Acad. Sci. USA*, **99**, 3099–3104.
20. Asher, G., Lotem, J., Sachs, L., Kahana, C. and Shaul, Y. (2002) Mdm-2 and ubiquitin-independent p53 proteasomal degradation regulated by NQO1. *Proc. Natl Acad. Sci. USA*, **99**, 13125–13130.
21. Bennett, K.L., Mester, J. and Eng, C. (2010) Germline epigenetic regulation of KILLIN in Cowden and Cowden-like syndrome. *JAMA*, **304**, 2724–2731.
22. Bayley, J.P. (2011) Succinate dehydrogenase gene variants and their role in cowden syndrome. *Am. J. Hum. Genet.*, **88**, 674–675.
23. Ng, P.C. and Henikoff, S. (2006) Predicting the effects of amino acid substitutions on protein function. *Annu. Rev. Genomics Hum. Genet.*, **7**, 61–80.
24. Ni, Y. and Eng, C. (2011) Response to bayley: functional study informs bioinformatic analysis. *Am. J. Hum. Genet.*, **88**, 676.
25. Warburg, O. (1956) On the origin of cancer cells. *Science*, **123**, 309–314.
26. Zundel, W., Schindler, C., Haas-Kogan, D., Koong, A., Kaper, F., Chen, E., Gottschalk, A.R., Ryan, H.E., Johnson, R.S., Jefferson, A.B. *et al.* (2000) Loss of PTEN facilitates HIF-1-mediated gene expression. *Genes Dev.*, **14**, 391–396.
27. Zhong, H., Chiles, K., Feldser, D., Laughner, E., Hanrahan, C., Georgescu, M.M., Simons, J.W. and Semenza, G.L. (2000) Modulation of hypoxia-inducible factor 1alpha expression by the epidermal growth factor/phosphatidylinositol 3-kinase/PTEN/AKT/FRAP pathway in human prostate cancer cells: implications for tumor angiogenesis and therapeutics. *Cancer Res.*, **60**, 1541–1545.
28. Yankovskaya, V., Horsefield, R., Tornroth, S., Luna-Chavez, C., Miyoshi, H., Leger, C., Byrne, B., Cecchini, G. and Iwata, S. (2003) Architecture of succinate dehydrogenase and reactive oxygen species generation. *Science*, **299**, 700–704.
29. Hinkle, P.C., Butow, R.A., Racker, E. and Chance, B. (1967) Partial resolution of the enzymes catalyzing oxidative phosphorylation. XV. Reverse electron transfer in the flavin-cytochrome beta region of the respiration chain of beef heart submitochondrial particles. *J. Biol. Chem.*, **242**, 5169–5173.
30. Ishii, T., Yasuda, K., Akatsuka, A., Hino, O., Hartman, P.S. and Ishii, N. (2005) A mutation in the SDHC gene of complex II increases oxidative stress, resulting in apoptosis and tumorigenesis. *Cancer Res.*, **65**, 203–209.
31. He, X., Ni, Y., Wang, Y., Romigh, T. and Eng, C. (2011) Naturally occurring germline and tumor-associated mutations within the ATP-binding motifs of PTEN lead to oxidative damage of DNA associated with decreased nuclear p53. *Hum. Mol. Genet.*, **20**, 80–89.
32. Klungland, A., Rosewell, I., Hollenbach, S., Larsen, E., Daly, G., Epe, B., Seeberg, E., Lindahl, T. and Barnes, D.E. (1999) Accumulation of premutagenic DNA lesions in mice defective in removal of oxidative base damage. *Proc. Natl Acad. Sci. USA*, **96**, 13300–13305.
33. Jackson, A.L. and Loeb, L.A. (2001) The contribution of endogenous sources of DNA damage to the multiple mutations in cancer. *Mutat. Res.*, **477**, 7–21.
34. Johnson, T.M., Yu, Z.X., Ferrans, V.J., Lowenstein, R.A. and Finkel, T. (1996) Reactive oxygen species are downstream mediators of p53-dependent apoptosis. *Proc. Natl Acad. Sci. USA*, **93**, 11848–11852.
35. Compton, S., Kim, C., Griner, N., Potluri, P., Scheffler, I.E., Sen, S., Jerry, D.J., Schneider, S. and Yadava, N. (2011) Mitochondrial dysfunction impairs tumor suppressor p53- expression/function. *J. Biol. Chem.*, **286**, 20297–20312.
36. Brooks, C.L. and Gu, W. (2006) p53 ubiquitination: Mdm2 and beyond. *Mol. Cell*, **21**, 307–315.
37. Gong, X., Kole, L., Iskander, K. and Jaiswal, A.K. (2007) NRH:quinone oxidoreductase 2 and NAD(P)H:quinone oxidoreductase 1 protect tumor suppressor p53 against 20s proteasomal degradation leading to stabilization and activation of p53. *Cancer Res.*, **67**, 5380–5388.
38. Tsvetkov, P., Reuven, N. and Shaul, Y. (2010) Ubiquitin-independent p53 proteasomal degradation. *Cell Death Differ.*, **17**, 103–108.
39. Eng, C. (2000) Will the real Cowden syndrome please stand up: revised diagnostic criteria. *J. Med. Genet.*, **37**, 828–830.
40. McWhinney, S.R., Pilarski, R.T., Forrester, S.R., Schneider, M.C., Sarquis, M.M., Dias, E.P. and Eng, C. (2004) Large germline deletions of mitochondrial complex II subunits SDHB and SDHD in hereditary paraganglioma. *J. Clin. Endocrinol. Metab.*, **89**, 5694–5699.
41. Mutter, G.L., Lin, M.C., Fitzgerald, J.T., Kum, J.B., Baak, J.P., Lees, J.A., Weng, L.P. and Eng, C. (2000) Altered PTEN expression as a diagnostic marker for the earliest endometrial precancers. *J. Natl Cancer Inst.*, **92**, 924–930.
42. Weng, L.P., Brown, J.L., Baker, K.M., Ostrowski, M.C. and Eng, C. (2002) PTEN blocks insulin-mediated ETS-2 phosphorylation through MAP kinase, independently of the phosphoinositide 3-kinase pathway. *Hum. Mol. Genet.*, **11**, 1687–1696.